Proton Exchange Membrane Fuel Cells: Effects of Gas Diffusion Layer Porosity Differences

Kaoutar Kabouchi[1*] and *Mohamed Karim* Ettouhami[1]

[1]Equipe de modélisation des structures et systèmes mécaniques, Mohammed V University in Rabat, ENSAM, Rabat, Morocco

Abstract. Fuel cells are a key technology for clean energy production due to their low environmental impact and their high efficiency, yet optimizing their performance remains challenging, particularly regarding the gas diffusion layer (GDL). The GDL is critical for distributing reactants and removing products within the cell. This study employs a 3D model, built in COMSOL Multiphysics, to simulate and assess fuel cell performance at different GDL porosity levels. The porosity varied from 0.2 to 0.8 in increments of 0.1, while all other material properties were kept constant. The results show that increasing porosity improves performance, with a strong correlation between simulation and experimental data. Polarization curves highlight the effect of GDL porosity on cell efficiency. This model offers valuable insights for optimizing fuel cell designs by adjusting GDL properties, contributing to the development of more efficient, cost-effective, and durable fuel cells for clean energy applications.

1 Introduction

Fuel cells are electrochemical systems that transform chemical energy directly into electrical power [1-5]. The basic principle involves the oxidation of H_2 at the anode and reduction of O_2 from the air at the cathode, with an electrolyte facilitating ion transport between them [6-9]. This process generates electricity, heat, and water as byproducts, without the harmful emissions typical of fossil fuel combustion [10-14]. Fuel cells can be employed in various applications, from portable electronics to stationary power generation and vehicle propulsion systems [15-20]. Their efficiency, environmental benefits, and versatility make them a promising technology in the transition towards sustainable energy solutions [21-24].

The Proton Exchange Membrane Fuel Cell (PEMFC) is a type of fuel cell that operates at relatively low temperatures, typically around 80°C [25-27]. It consists of an electrolyte membrane, usually made of a per-fluorinated sulfonic acid polymer, which selectively allows protons to pass through while blocking e^-. This membrane is sandwiched between two electrodes: the anode and the cathode. At the anode, hydrogen gas is supplied and catalytically split into H^+ and e^-. The H^+ migrate through the membrane to the cathode, while the e^- travel through an external circuit, generating electricity. At the cathode, O_2 (usually from the air) reacts with the H^+ and e^- to form H_2O, the main byproduct [28-32]. PEMFCs

* Corresponding author: kaoutar_kabouchi@um5.ac.ma

are known for their efficiency in converting chemical energy directly into electrical energy, making them suitable for various applications [33-37]. Quick start-up, compact size, and low emissions are key advantages of PEMFCs. However, challenges like membrane cost and durability are still under research [38-40]. Figure 1 shows schematic design of the PEMFC.

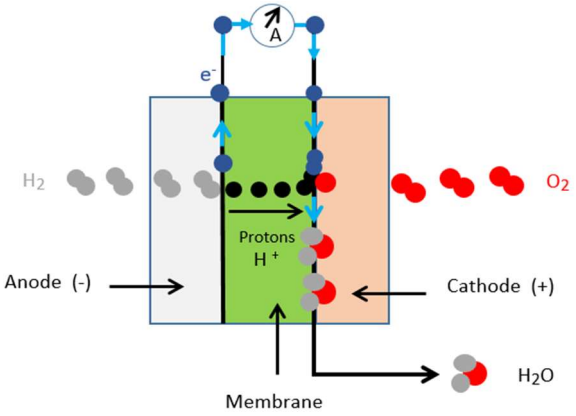

Fig. 1. Schematic design of the PEMFC.

Polarization curves are frequently used in evaluating fuel cell performance to illustrate how cell voltage correlates with current density [41, 42]. Figure 2 illustrates a typical current-voltage relationship, known as the polarization curve, for a single PEMFC. This graph displays how the voltage varies with different levels of current output. To ensure fair comparison across PEMFCs of varying sizes and outputs, the current density ($A.cm^{-2}$) is used to normalize the current values. In theory, a fuel cell should provide any required current while keeping the thermodynamically required voltage constant, assuming sufficient fuel supply. However, practical fuel cells inevitably operate below the ideal reversible voltage due to various losses. As current draw increases, the cell's voltage output decreases, thereby limiting the total available power. Maintaining high cell voltage under load is challenging, as depicted in Figure 2 where operational voltage falls short of the reversible voltage due to irreversible losses. These losses increase with higher currents and encompass activation loss, ohmic loss, mass transport or concentration loss, as well as losses because of internal currents and fuel crossover [43-46]. Activation loss arises from slow reactions within the catalyst layer (CL), where voltage is expended to drive electrochemical reactions involving electrons and protons [47]. Figure 2 highlights this with an initial sharp voltage drop, indicating the threshold at which sufficient electron and proton accumulation allows continuous reaction with adequate gas supply.

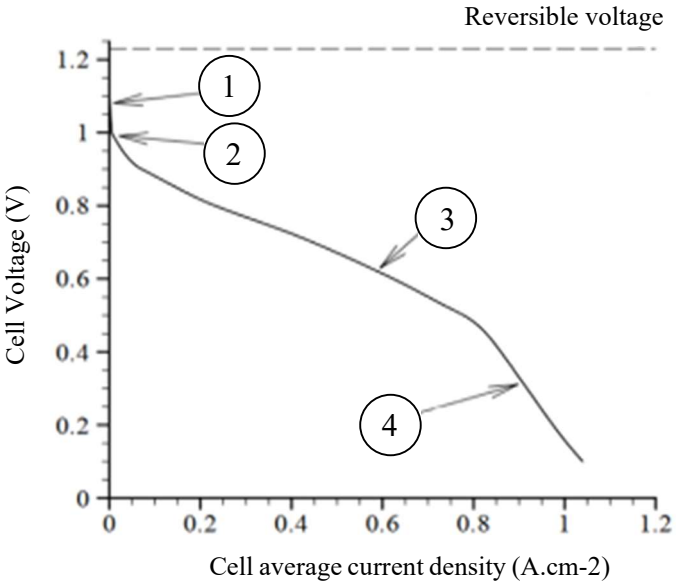

Fig. 2. Polarization curve sample for a single PEMFC (1: Fuel crossover and internal currents cause the open circuit voltage to be lower than the reversible voltage, 2: Voltage decreases quickly at first, mostly as a result of activation loss, 3: Ohmic loss is the primary cause of the voltage's slow and linear decrease, 4: Mostly as a result of concentration loss, voltage decreases more quickly at high currents).

The ohmic loss in a fuel cell refers to the resistance encountered by electrons and protons as they move through the membranes, electrodes, and interconnections. This resistance causes a voltage decrease that is directly in proportion to the current density, as illustrated by the linear decline in performance shown in Figure 2 [48]. Mass transport, or concentration loss, occurs due to changes in reactant concentration within the CL as reactants are consumed from inlet to outlet along the flow channel. This change in concentration affects voltage through alterations in reactant partial pressures, hence it's termed concentration loss. It also relates to mass transport loss, as insufficient reactant delivery to the CL results in concentration reduction [49]. In Figure 2, concentration loss manifests at high current densities with a steep voltage drop, reflecting how adequate reactant supply controls current output. Fuel crossover and internal currents describe reactant passage and electron conduction through the membrane, respectively [50]. Though membranes ideally transport only ions, small amounts of reactant and electrons can still permeate, notably affecting the open circuit voltage in low-temperature fuel cells, which typically falls short of the reversible voltage because of these losses. However, these losses diminish significantly under load, as current draw enhances reactant utilization. The PEMFC operating voltage at various current densities is calculated by subtracting irreversibility-induced voltage losses from the reversible voltage. Specifically, open circuit voltage equals reversible voltage minus losses from internal currents and fuel crossover, establishing a relationship between open circuit voltage (V_{open}) and operating voltage (V_{cell}):

$$V_{cell} = V_{open} - \eta_{act} - \eta_{ohm} - \eta_{conc} \quad (1)$$

The performance of fuel cells has been studied extensively. Researchers have used both experimental methods and computational models to explore various factors influencing their efficiency [51-54]. Several studies have explored the influence of GDL characteristics, such as material type, porosity, and thickness, on the performance of PEMFCs. The GDL plays a

crucial role in facilitating the transport of reactant gases, managing water produced during the reaction, and maintaining electrical conductivity between the catalyst layer and the current collectors. For instance, researchers including Akiki et al., [55] proposed various fuel cell models to investigate the compression impact on fuel cells. Their findings highlighted that mechanical requirement affect parameters such as GDL porosity, permeability, and pressure at the GDL/Bipolar plate interface, contact resistance between GDL and BP, and GDL conductivity. These parameters cannot remain constant in PEMFC modeling. Yuan et al., [56] conducted a three-dimensional model for PEMFC, examining mass transfer and thermal along with cell performance in the thread/chamfer structure of the GDL at various pressures. They indicated that compression directly influences porosity distribution, resulting in non-uniform porosity across the chamfer width. Zamel et al., [57] have shown that carbon cloth tends to offer better water management and gas permeability than carbon paper, which leads to improved overall fuel cell performance, particularly at high current densities. Litster and McLean [58] have highlighted the trade-off between increasing GDL thickness to enhance water retention and minimizing thickness to reduce resistance to gas transport, indicating that intermediate thickness values often yield the best performance.
The study of PEMFC performance is highly beneficial in energy research and essential for the progression of fuel cell technology.
In this study, a three-dimensional mathematical model is developed to evaluate the PEMFC performance by examining how different levels of GDL porosity impact its performance, aiding in the comprehension of the PEMFC's internal behavior.

2 Methodology

2.1 Geometric model

Figure 3 depicts a 3D model of PEMFC. The model comprises seven zones.

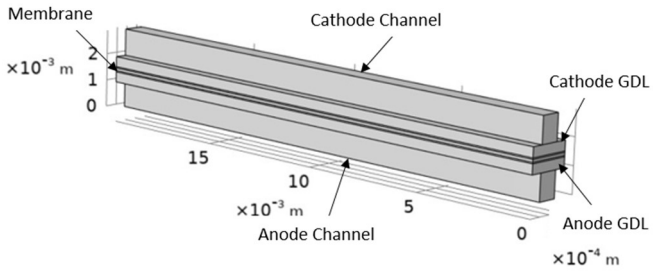

Fig. 3. Three-dimensional modelling of the PEMFC.

For our model, the subsequent geometric parameters were applied:
Length of cell of 0.02 m, height of channel of 1.1 e^{-3} m, width of channel of 0.7874 e^{-3} m, rib width of 0.90932 e^{-3} m, GDL width 380 e^{-6} m, membrane thickness 100 e^{-6} m and porous electrode thickness 50 e^{-6} m.

2.2 Basic assumptions

Assumptions including 3D domain, stationary model, all gases are assumed to behave ideally, laminar flow due to small pressure, incompressible fluid, cell temperature is held constant, membrane is impermeable to reactant species, GDL exhibits isotropic and homogeneous materials were made.

2.3 Governing equations

The following summarizes the conservation of electric charge, continuity, and Maxwell-Stefan mathematical expressions [59]:

Maxwell-Stefan equation:

$$\nabla.\left\{-\rho\omega_i \sum_{j=1}^{n} D_{ij}\left[\frac{M}{M_j}\left(\nabla\omega_j + \omega_j\frac{\nabla M}{M}\right) + (x_j - \omega_j)\frac{\nabla P}{P}\right] + \rho\omega_i u\right\} = R_i \quad (2)$$

Continuity equation:

$$\nabla(\rho u) = S \quad (3)$$

Conservation of electric charge:

$$\nabla.(-\sigma_s\nabla.\phi_s) = S_s \quad (4)$$
$$\nabla.(-\sigma_m\nabla.\phi_m) = S_m \quad (5)$$

Where D is coefficient of diffusion, M is mass of molecules, P is pressure, R is source expression resulting from chemical reactions, S is current source term, u is vector of velocity, x is molar fraction, ϕ is potential, σ is electric conductivity, ω is mass fraction, ρ is density, μ is viscosity in dynamic, subscript i is particular species of H_2 and H_2O (anode), subscript j is particular species of O_2, H_2O, and N_2 (cathode), subscript s is solid phase and subscript m is membrane.

2.4 Boundary conditions

The boundary conditions for the model in this study are as follows:
- In a time-dependent research, velocity and temperature are established at the channel inlet, and a step function is utilized to calculate these two parameters,
- Continuity at all internal boundaries,
- All channel walls have no slip boundary condition,
- All initial values set to zero,
- Constrain outer edges set to zero for both inlet and outlet,
- Convective flux boundary conditions were used, and there was no backpressure at the channel's outlet,
- PEMFC has environmental insulation.

The specific parameter values used in this study are provided in Section "Numerical procedure".

3 Numerical procedure

For the model's geometry, a structured grid (Figure 4) is created using the COMSOL Multiphysics software. The mesh included a total of 19708 elements of domains, 7392 elements of boundaries, and 972 elements of edges. Boundary conditions from COMSOL were applied to solve the mathematical equations, and a methodology established on the method of finite elements was utilized. The structure was run under temperature of 333.15 K.
The characteristics of the 3D model's mesh are listed in Table 1.

Table 1. Characteristics of the mesh.

Mesh characteristics	**Value**
Maximum element size	0.001
Minimum element size	1.8e-4
Resolution of curvature	0.6
Resolution of Narrow regions	0.5
Maximum elemental growth rate	1.5

Table 2 reports the physicochemical characteristics developed in this structure.

Table 2. Physicochemical parameters.

Description	**Value**
GDL porosity	0.4
GDL permeability	1.18e-11 m^2
GDL electric conductivity	222 $S.m^{-1}$
Reference concentration of O_2	40.88 $mol.m^{-3}$
Reference concentration of H_2	40.88 $mol.m^{-3}$
Membrane conductivity	9.82 $S.m^{-1}$
Specific surface area	1e7 m^{-1}
Inlet flow velocity (anode)	0.10352 $m.s^{-1}$
Inlet flow velocity (cathode)	0.41078 $m.s^{-1}$
Viscosity (anode)	1.19e-5 Pa.s
Viscosity (cathode)	2.46e-5 Pa.s
Inlet mass fraction of H_2 (anode)	0.963
Inlet mass fraction of O_2 (cathode)	0.202
Inlet mass fraction of H_2O	0.037

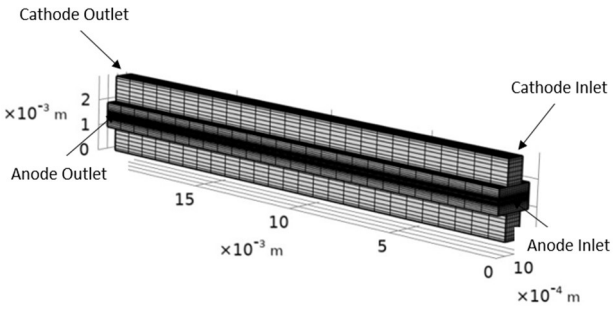

Fig. 4. Structure after meshing.

4 Results and discussions

4.1 Model validation

In order to evaluate the model precision, we carried out an investigation. Compared its findings, with an experimental study conducted by Martin Bates [60] as depicted in Figure 5. We thoroughly examined the polarization curve in both the activation and ohmic areas and our outcomes using COMSOL Multiphysics exhibited a resemblance to those obtained in the study barring a slight deviation, at 0.55 A/cm^2 (Figure 5). However, we observed that at high current densities, the model is unable to replicate the experimental results. The liquid water presence in the catalyst and gas diffusion layers might be the cause of this discrepancy.

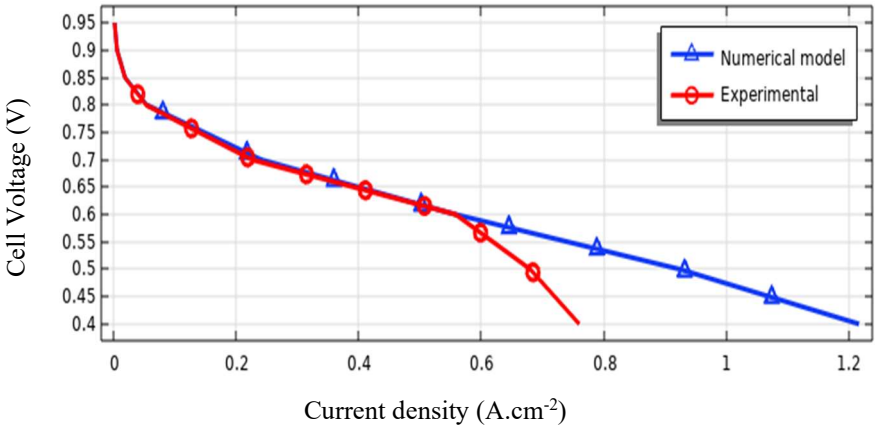

Fig. 5. Contrasting present modeling results against experimental data.

4.2 Simulation result

The correlation between GDL porosity and PEMFC performance characteristics is illustrated in Figure 6. Seven different porosity values were used in the simulations: the base case value of 0.4, along with 0.2, 0.3, 0.5, 0.6, 0.7, and 0.8. Figure 6 demonstrates that increased porosities in GDL result in higher voltages at output, especially at higher cell current densities. Notably, the value of 0.1 yields the lowest polarization curve among those shown in Figure 6, suggesting that reactant flow through the GDL may be restricted at this porosity

level, leading to reduced concentration of H^+ at the electrode and lower polarization. Conversely, curves that indicate increased GDL porosities (0.5, 0.6, 0.7, and 0.8) show closely aligned performance due to unhindered reactant flow. Therefore, porosity values of 0.4 and 0.6 in the GDL have minimal impact on performance curves for PEMFC. Furthermore, as depicted in Figure 6, GDL porosity has minimal impact on increased voltages at operation. But, at lower voltages, especially as water formation increases with higher current densities, delivering oxidant to the cathode catalyst becomes more challenging. While the anode side experiences sufficient reactions, only partial reactions occur on the fuel cell cathode side because the water obstructs O_2, leading to a faster decline in lower porosity fuel cell performance. This underscores the significance of selecting optimal porosity values for the chosen GDL materials to enhance PEMFC performance. The results showed that increasing porosity improves oxygen flow, enhancing performance, especially at higher current densities. However, the mechanical integrity of the GDL becomes a concern with porosity above 0.8, as it could lead to structural failures under operational stresses. Values above 0.6 do not yield significant performance improvements because oxygen transport has already reached an optimal balance at these levels. Beyond this point, the diminishing returns in performance may result from water flooding, which limits the effective use of additional oxygen supply. At higher current densities, ohmic and mass transport losses become more pronounced. Ohmic losses could be mitigated by selecting materials with higher conductivity for both the GDL and the membrane. For mass transport losses, incorporating materials with optimal pore sizes that balance reactant diffusion and water management is crucial. Additionally, advanced GDL designs, such as those with graded porosity, could help alleviate concentration losses by maintaining efficient reactant distribution. While higher porosity enhances oxygen distribution and performance at high current densities, there is a trade-off with mechanical stability. A porosity above 0.8 could indeed compromise the structural integrity of the GDL, leading to potential durability issues [61].

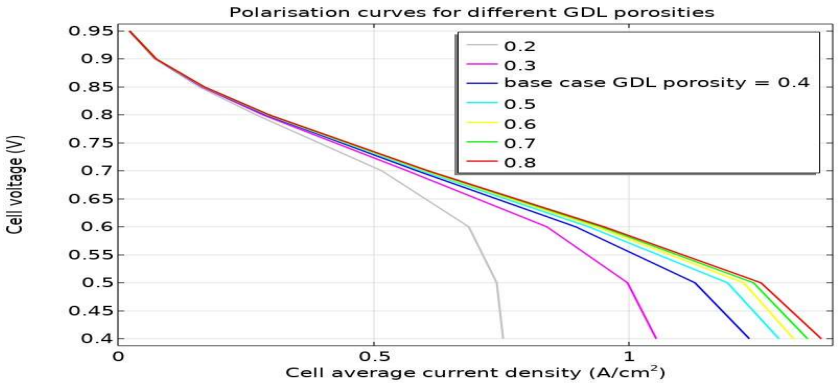

Fig. 6. Comparison of polarization curves across various GDL porosities.

4.3 Distribution of oxygen on the cathode side under different values of porosity

Figures 7-13 show the partial mass of O_2 on the cathode side, which changes with porosity values while the fuel cell functions at 0.5 V. These figures indicate that water creation in the channel as a result of the reaction rate in the middle region limits O_2 delivery to that location, similar to how porosity impacts oxygen distribution. This decrease is more noticeable when the GDL porosity is low. This happens because low porosity GDL presents a high physical barrier to oxygen, which causes it to pass through the cathode flow channel instead of

diffusing into the GDL. It is thought that this phenomenon is the main reason why fuel cell performance has declined. For more clarification, the figures show how oxygen distribution is affected by varying GDL porosity levels, directly impacting the fuel cell's performance. Specifically, in low porosity GDLs, oxygen diffusion is restricted, which leads to localized oxygen starvation at the cathode catalyst layer. This lack of oxygen supply causes mass transport losses, which manifest as voltage drops, particularly at higher current densities. As the GDL porosity increases, oxygen is more uniformly distributed, improving overall fuel cell performance by reducing these losses. This relationship is critical to understanding how optimizing GDL porosity can help maintain higher voltages and cell efficiency under varying operating conditions. Based on the findings, the optimal GDL porosity for transportation applications (where dynamic conditions require higher performance and rapid response) would range from 0.6 to 0.8. This range provides sufficient oxygen distribution and reduces the impact of water buildup, which is critical for high-power and efficiency needs. However, for stationary power applications, where durability and long-term operation are more important, a lower porosity between 0.4 and 0.6 may be ideal. This range provides a balance between performance and mechanical stability, ensuring longevity in less demanding operating environments. For GDLs with higher porosity values (such as those used in transportation applications), carbon fiber-based materials or woven carbon composites are recommended for their superior durability and flexibility. These materials maintain structural integrity even at high porosity. Additionally, advanced manufacturing techniques like chemical vapor deposition (CVD) or electrospinning can be used to produce GDLs with tailored porosity and high precision, ensuring optimal performance while considering cost and scalability.

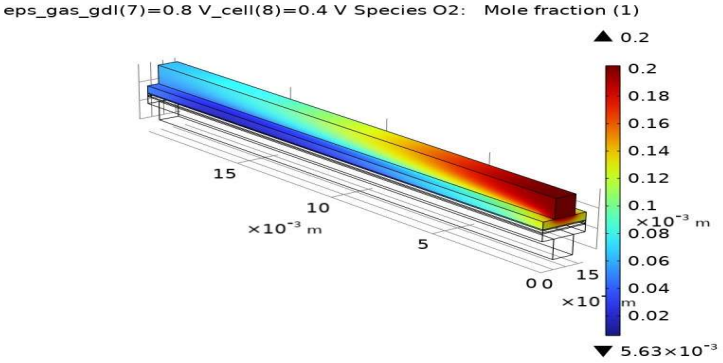

Fig. 7. Variation of O_2 distribution for the porosity of 0.8.

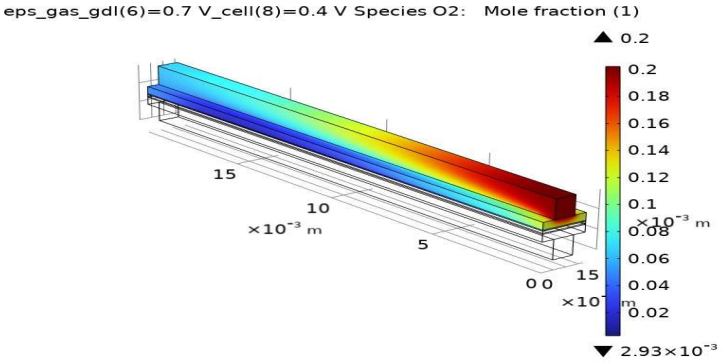

Fig. 8. Variation of O_2 distribution for the porosity of 0.7.

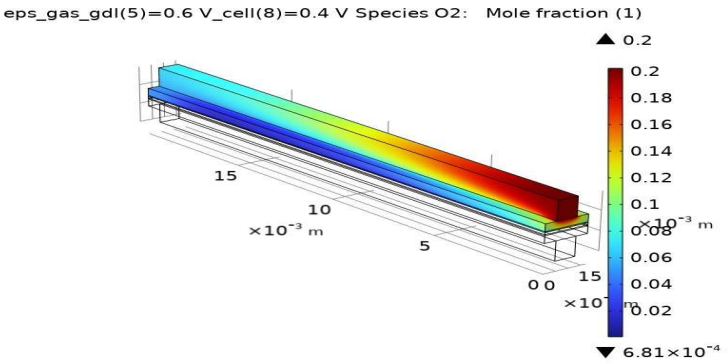

Fig. 9. Variation of O_2 distribution for the porosity of 0.6.

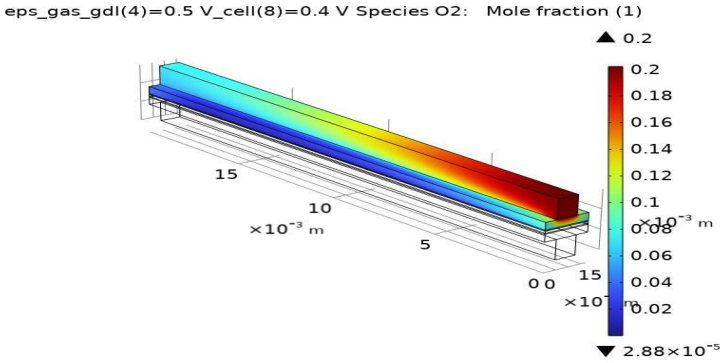

Fig. 10. Variation of O_2 distribution for the porosity of 0.5.

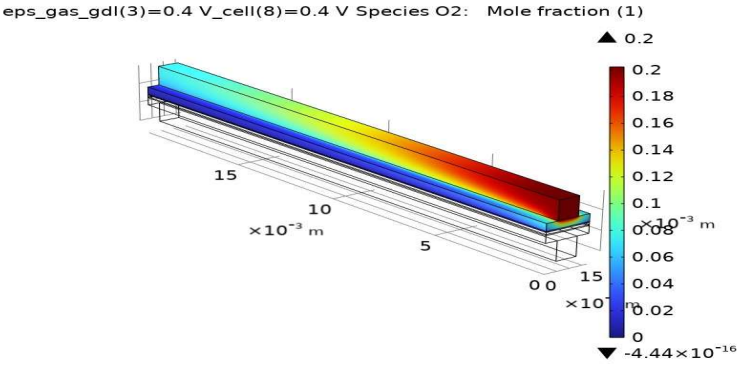

Fig. 11. Variation of O_2 distribution for the porosity of 0.4.

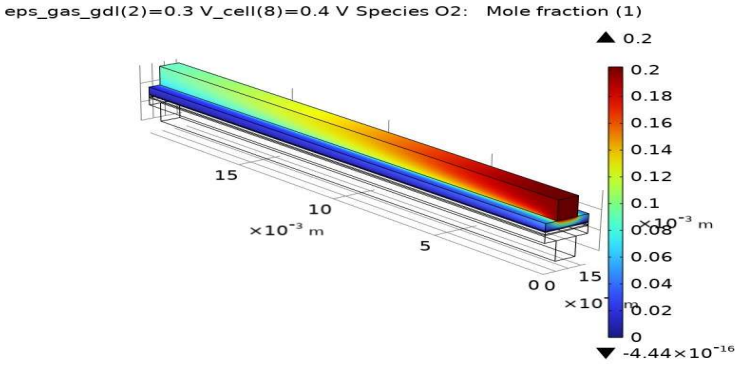

Fig. 12. Variation of O_2 distribution for the porosity of 0.3.

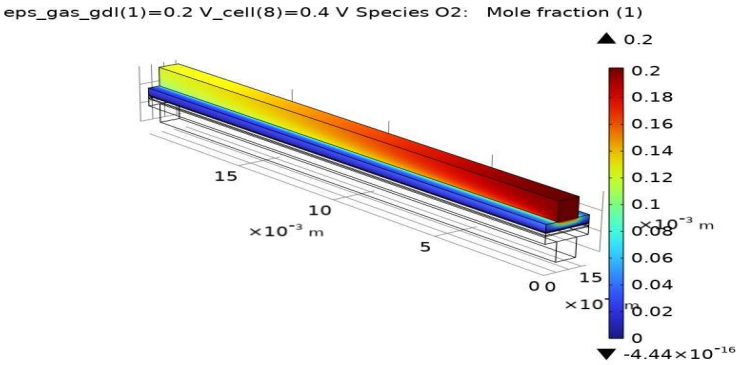

Fig. 13. Variation of O_2 distribution for the porosity of 0.2.

5 Conclusions

In conclusion, a study utilizing the COMSOL Multiphysics software was executed to evaluate the varying GDL porosity effect on PEMFCs. With the GDL exception, all geometric parameters and material properties were maintained constant in the developed model. The GDL porosity was studied parametrically, with modifications made in 0.1 increments, and the range of values was 0.2 to 0.8. The simulation results showed a good agreement with published experimental data. Also, the polarization curves were used to assess the PEMFC's performance. It is discovered that as the GDL porosity increases from 0.2 to 0.8, the cell's performance gets better. In addition, the study reveals that porosity impacts oxygen distribution, causing reduced water production and lower oxygen delivery in the central region due to reaction rates. This effect is particularly significant when the GDL has low porosity, creating high physical resistance that redirects oxygen flow through the cathode channel instead of diffusing into the GDL, thereby reducing fuel cell performance. This research can contribute to optimizing the PEMFCs design and performance by providing insights into the critical role of gas diffusion layer porosity. The study demonstrates that higher porosity levels in the GDL improve PEMFC performance, particularly at higher current densities. However, while this research has provided valuable insights into optimizing GDL porosity for better reactant distribution, future research could explore the integration of two-phase flow models to capture the effects of liquid water accumulation more accurately.

Potential future work includes extending the model to account for non-ideal conditions, such as temperature and pressure fluctuations or varying humidity levels. Furthermore, investigating the mechanical stability of highly porous GDLs and their impact on long-term durability would provide deeper insights into the trade-offs between performance and structural integrity. Real-world applications of this research lie in the development of more efficient and cost-effective PEMFCs for electric vehicles and stationary power systems, where optimizing the GDL could lead to reduced material costs and improved operational efficiency. Consideration of manufacturing limitations and cost factors in selecting optimal porosity values will also play a crucial role in scaling these findings to commercial applications.

References

1. F. Jiang, X. Yuan, L. Hu, G. Xie, Z. Zhang, X. Li, H. Wang, A comprehensive review of energy storage technology development and application for pure electric vehicles. J. Energy Storage **86**, 111159-111184 (2024)
2. K. Najeeb, A. H. Tariq, M. Hassan, M. Anwar, A. Bahadar, S. A. A. Kazmi, M. Yousif, Techno-economic and performance assessment of a hybrid fuel cell-based combined heat and power system for dairy industry. Environ. Dev. Sustain., 1-29 (2024)
3. N. Twi-Yeboah, D. Osei, M. K. Danquah, Advances in solar-derived chemical fuel systems. Energies **16**, 2864-2884 (2023)
4. B. B. P. Solis, J. C. C. Argüello, I. M. Canche, L. G. Barba, M. P. Gurrola, CFD Analysis in the Mesh Modified Gas Diffusion Layer of a Proton Exchange Membrane Fuel Cell (PEMFC). CFD Lett. **16**, 55-67 (2024)
5. K. Kabouchi, M. K. Ettouhami, H. Mounir, K. Elbikri, Performance Investigation of PEM Fuel Cell with Three-Pass Serpentine Flow Fields under Varying Operating Voltages. CFD Lett. **16**, 54-63 (2024)
6. S. P. S. Badwal, S. Giddey, A. Kulkarni, J. Goel, S. Basu, Direct ethanol fuel cells for transport and stationary applications–A comprehensive review. Appl. Energy **145**, 80-103 (2015)
7. C. W. Anson, S. S. Stahl, Mediated Fuel Cells: Soluble Redox Mediators and Their Applications to Electrochemical Reduction of O2 and Oxidation of H2, Alcohols, Biomass, and Complex Fuels. Chem. Rev. **120**, 3749-3786 (2020)
8. W. Zhou, S. Chen, X. Meng, J. Li, J. Gao, Energy-saving cathodic H2 production enabled by non-oxygen evolution anodic reactions: a critical review on fundamental principles and applications. Int. J. Hydrogen Energy. **48**, 15748-15770 (2023)
9. Z. Qiao, B. Lin, H. Zhang, Y. Yan, L. Li, J. Tang, T. Zhou, Cathode and anode catalysis mechanism and design principle of water all splitting in chlorinated neutral environment: A review. Int. J. Hydrogen Energy. **63**, 1182-1196 (2024)
10. P. J. Megía, A. J. Vizcaíno, J. A. Calles, A. Carrero, Hydrogen production technologies: from fossil fuels toward renewable sources. A mini review. Energy & Fuels **35**, 16403-16415 (2021)
11. G. A. Ryabov, Chemical looping combustion and gasification of fuels. A review of studies and new process solutions. Therm. Eng. **69**, 26-41 (2022)
12. A. Shamoon, A. Haleem, S. Bahl, M. Javaid, S. B. Garg, R. C. Sharma, J. Garg, Environmental impact of energy production and extraction of materials-a review. Mater. Today Proc. **57**, 936-941 (2022)

13. L. Cherwoo, I. Gupta, G. Flora, R. Verma, M. Kapil, S. K. Arya, V. Ashokkumar, Biofuels an alternative to traditional fossil fuels: A comprehensive review. Sustain. Energy Technol. Assess. **60**, 103503-103514 (2023)
14. Y. Wang, Y. Liu, Z. Xu, K. Yin, Y. Zhou, J. Zhang, Z. Zhu, A review on renewable energy-based chemical engineering design and optimization. Renew. Sustain. Energy Rev. **189**, 114015-114034 (2024)
15. A. Pramuanjaroenkij, S. Kakaç, The fuel cell electric vehicles: The highlight review. Int. J. Hydrogen Energy. **48**, 9401-9425 (2023)
16. M. A. Aminudin, S. K. Kamarudin, B. H. Lim, E. H. Majilan, M. S. Masdar, N. Shaari, An overview: Current progress on hydrogen fuel cell vehicles. Int. J. Hydrogen Energy. **48**, 4371-4388 (2023)
17. H. Chehrmonavari, A. Kakaee, S. E. Hosseini, U. Desideri, G. Tsatsaronis, G. Floerchinger, A. Paykani, Hybridizing solid oxide fuel cells with internal combustion engines for power and propulsion systems: A review. Renew. Sustain. Energy Rev. **171**, 112982-113003 (2023)
18. V. K. Visvanathan, K. Palaniswamy, D. Ponnaiyan, M. Chandran, T. Kumaresan, J. Ramasamy, S. Sundaram, Fuel cell products for sustainable transportation and stationary power generation: Review on market perspective. Energies **16**, 2748-2768 (2023)
19. Z. Wang, Z. Liu, L. Fan, Q. Du, K. Jiao, Application progress of small-scale proton exchange membrane fuel cell. Energy Reviews **2**, 100017-100028 (2023)
20. A. Parikh, M. Shah, M. Prajapati, Fuelling the sustainable future: a comparative analysis between battery electrical vehicles (BEV) and fuel cell electrical vehicles (FCEV). Environ. Sci. & Pollut. Res. **30**, 57236-57252 (2023)
21. F. O. Usman, E. C. Ani, W. Ebirim, D. J. P. Montero, K. A. Olu-lawal, N. Ninduwezuor-Ehiobu, Integrating renewable energy solutions in the manufacturing industry: challenges and opportunities: a review. Engineering Science & Technology Journal **5**, 674-703 (2024)
22. P. Simpa, N. O. Solomon, O. A. Adenekan, S. C. Obasi, Sustainable nanomaterials' role in green supply chains and environmental sustainability. Engineering Science & Technology Journal **5**, 1678-1694 (2024)
23. M. Aravindan, P. Kumar, Hydrogen towards sustainable transition: A review of production, economic, environmental impact and scaling factors. Results Eng., 101456-101476 (2023)
24. L. Zhang, C. Jia, F. Bai, W. Wang, S. An, K. Zhao, H. Sun, A comprehensive review of the promising clean energy carrier: Hydrogen production, transportation, storage, and utilization (HPTSU) technologies. Fuel **355**, 129455-129478 (2024)
25. N. A. Qasem, A recent overview of proton exchange membrane fuel Cells: Fundamentals, Applications, and advances. Appl. Therm. Eng. **252**, 123746-123774 (2024)
26. Z. Zhang, J. Mao, Z. Liu, Advancements and insights in thermal and water management of proton exchange membrane fuel cells: Challenges and prospects. Int. Commun. Heat Mass Transf. **153**, 107376-107393 (2024)
27. K. Li, J. Hong, C. Zhang, F. Liang, H. Yang, F. Ma, F. Wang, Health state monitoring and predicting of proton exchange membrane fuel cells: A review. J. Power Sources **612**, 234828-234841 (2024)

28. M. Odgaard, The use of per-fluorinated sulfonic acid (PFSA) membrane as electrolyte in fuel cells. Adv. Fluoride-Mater. Energy Convers., 325-374 (2015)
29. R. Gloukhovski, V. Freger, Y. Tsur, Understanding methods of preparation and characterization of pore-filling polymer composites for proton exchange membranes: a beginner's guide. Rev. Chem. Eng. **34**, 455-479 (2018)
30. J. Gao, X. Dong, Q. Tian, Y. He, Carbon nanotubes reinforced proton exchange membranes in fuel cells: An overview. Int. J. Hydrogen Energy. **48**, 3216-3231 (2023)
31. D. Henkensmeier, W. C. Cho, P. Jannasch, J. Stojadinovic, Q. Li, D. Aili, J. O. Jensen, Separators and Membranes for Advanced Alkaline Water Electrolysis. Chem. Rev. **124**, 6393-6443 (2024)
32. S. Joseph, Applications of Multifunctional Nanomaterials, 125-142 (2023)
33. M. M. Tellez-Cruz, J. Escorihuela, O. Solorza-Feria, V. Compañ, Proton exchange membrane fuel cells (PEMFCs): Advances and challenges. Polym. **13**, 3064-3117 (2021)
34. J. Lindorfer, D. C. Rosenfeld, H. Böhm, Fuel cells: Energy conversion technology. Future energy, 495-517 (2020)
35. R. G. Bodkhe, R. L. Shrivastava, V. K. Soni, R. B. Chadge, A review of renewable hydrogen generation and proton exchange membrane fuel cell technology for sustainable energy development. Int. J. Electrochem. Sci. **18**, 100108-100119 (2023)
36. E. Ogungbemi, T. Wilberforce, O. Ijaodola, J. Thompson, A. G. Olabi, Selection of proton exchange membrane fuel cell for transportation. Int. J. Hydrogen Energy. **46**, 30625-30640 (2021)
37. K. Kabouchi, M. K. Ettouhami, H. Mounir, Simulation Examination of the Impact of Operating Parameters on a High-Temperature Proton Exchange Membrane Fuel Cell. Math. Model. Eng. Probl. **11**, 1626-1632 (2024)
38. G. Wang, Y. Yu, H. Liu, C. Gong, S. Wen, X. Wang, Z. Tu, Progress on design and development of polymer electrolyte membrane fuel cell systems for vehicle applications: A review. Fuel Process. Technol. **179**, 203-228 (2018)
39. M. Pan, C. Pan, C. Li, J. Zhao, A review of membranes in proton exchange membrane fuel cells: Transport phenomena, performance and durability. Renew. Sustain. Energy Rev. **141**, 110771-110798 (2021)
40. F. Qureshi, M. Yusuf, H. Ibrahim, H. Kamyab, S. Chelliapan, C. Q. Pham, D. V. N. Vo, Contemporary avenues of the Hydrogen industry: Opportunities and challenges in the eco-friendly approach. Environ. Res. **229**, 115963-115984 (2023)
41. L. Zhao, J. Hong, J. Xie, S. Jiang, X. Wei, P. Ming, H. Dai, Investigation of local sensitivity for vehicle-oriented fuel cell stacks based on electrochemical impedance spectroscopy. Energy **262**, 125381-125397 (2023)
42. K. Meng, B. Chen, H. Zhou, W. Chen, Z. Tu, Experimentally investigation on current density distribution characteristics of hydrogen-oxygen proton exchange membrane fuel cells under dynamic loading. J. Clean. Prod. **393**, 136315-136330 (2023)
43. Y. Wang, Z. Lu, Y. Li, Z. Ma, Y. Gu, Q. Guo, Performance analysis and multi-optimization of direct methanol fuel cell based on a novel numerical model considering mass transfer. Int. J. Hydrogen Energy. **62**, 362-374 (2024)
44. F. Mazzeo, L. Di Napoli, M. Carello, Assessing Open Circuit Voltage Losses in PEMFCs: A New Methodological Approach. Energies **17**, 2785-2805 (2024)

45. K. Gunaseelan, S. Gajalakshmi, S. K. Kamaraj, J. Solomon, D. A. Jadhav, Electrochemical losses and its role in power generation of microbial fuel cells. Bioelectrochemical Systems: Vol. 1 Principles and Processes, 81-118 (2020)
46. L. S. Wang, S. M. Haile, From Fundamental Interfacial Reaction Kinetics to Macroscopic Current–Voltage Characteristics: Case Study of Solid Acid Fuel Cell Limitations and Possibilities. Adv. Mater. Interfaces, (2024)
47. M. Ma, L. Shen, Z. Zhao, P. Guo, J. Liu, B. Xu, Z. Wang, Activation methods and underlying performance boosting mechanisms within fuel cell catalyst layer. eScience, 100254-100276 (2024)
48. U. Mitra, A. Arya, S. Gupta, A comprehensive and comparative review on parameter estimation methods for modelling proton exchange membrane fuel cell. Fuel **335**, 127080-127116 (2023)
49. J. Guo, P. Brimley, M. J. Liu, E. R. Corson, C. Muñoz, W. A. Smith, W. A. Tarpeh, Mass transport modifies the interfacial electrolyte to influence electrochemical nitrate reduction. ACS Sustain Chem Eng **11**, 7882-7893 (2023)
50. E. Eikeng, A. Makhsoos, B. G. Pollet, Critical and strategic raw materials for electrolysers, fuel cells, metal hydrides and hydrogen separation technologies. Int. J. Hydrogen Energy. **71**, 433-464 (2024)
51. S. Zaman, L. Huang, A. I. Douka, H. Yang, B. You, B. Y. Xia, Oxygen reduction electrocatalysts toward practical fuel cells: progress and perspectives. Angew. Chem. Int. Ed. **133**, 17976-17996 (2021)
52. G. Fazio, L. Ferrighi, D. Perilli, C. Di Valentin, Computational electrochemistry of doped graphene as electrocatalytic material in fuel cells. Int. J. Quantum Chem. **116**, 1623-1640 (2016)
53. B. Wu, X. Xu, G. Dong, M. Zhang, S. Luo, D. Y. Leung, Y. Wang, Computational modeling studies on microfluidic fuel cell: A prospective review. Renew. Sustain. Energy Rev. **191**, 114082-114109 (2024)
54. M. Sarker, M. A. Rahman, F. Mojica, S. Mehrazi, W. J. Kort-Kamp, P. Y. A. Chuang, Experimental and computational study of the microporous layer and hydrophobic treatment in the gas diffusion layer of a proton exchange membrane fuel cell. J. Power Sources **509**, 230350-230360 (2021)
55. T. Akiki, G. Accary, W. Charon, R. Kouta, Influence of local porosity, local permeability, and contact resistance between the gas diffusion layer and the bipolar plate, on the performances of a polymer electrolyte membrane fuel cell. CCCA12, 1-6 (2012, December)
56. J. Wang, J. Yuan, B. Sundén, Modeling of inhomogeneous compression effects of porous GDL on transport phenomena and performance in PEM fuel cells. Int. J. Energy Res. **41**, 985-1003 (2017)
57. N. Zamel, X. Li, J. Shen, Numerical estimation of the effective electrical conductivity in carbon paper diffusion media. Appl. Energy **93**, 39-44 (2012)
58. S. Litster, G. J. J. O. P. S. McLean, PEM fuel cell electrodes. J. Power Sources **130**, 61-76 (2004)
59. E. U. Ubong, Z. Shi, X. Wang, Three-dimensional modeling and experimental study of a high temperature PBI-based PEM fuel cell. J. Electrochem. Soc. **156**, 10 (2009)
60. A. M. Bates, University of Louisville (2015)
61. S. Park, J. W. Lee, B. N. Popov, A review of gas diffusion layer in PEM fuel cells: Materials and designs. Int. J. Hydrogen Energy. **37**, 5850-5865 (2012)